

A PLANAR ANISOTROPIC YIELD FUNCTION BASED ON MULTI AXIAL STRESS STATES IN FINITE ELEMENTS.

B.D. Carleer¹, T. Meinders¹, H.H.Pijlman¹, J. Huétink¹, H. Vegter²

¹ University of Twente, Faculty of Mechanical Engineering, P.O.Box 217, Enschede, NL

² Hoogovens R&D, Product Application Centre, P.O.Box 10000, Ijmuiden, NL

Abstract. A new material description based on multi axial stress states has been developed. The material description has been introduced for the planar isotropic case. Based on the isotropic case the description is extended to a planar anisotropic description. The Limiting Dome Height test is used to examine the material description. Both the strain distribution and the punch height at failure are very well described with the new material description.

1. INTRODUCTION

In simulation models for sheet metal forming, the plastic behaviour of the material at multi-axial stress states is commonly described with a quadratic Hill yield function [1]. The parameters in the Hill yield function are determined with uni-axial tensile tests. This description of the plastic material behaviour is not always sufficiently accurate. Therefore, a yield function based on multi-axial stress states measurements is necessary.

Vegter [2] proposed a description which directly uses the experimental results at multi-axial stress states. A four point interpolation method has been developed based on the pure shear point, the uni-axial point, the plane strain point and the equi-bi-axial point. These reference points are represented in the principal stress space, see Figure 1. A plane stress state is assumed.

In case of planar isotropic material behaviour the gradient $d\sigma_1/d\sigma_2$ at the reference points is known. In the uni-axial point the gradient is a function of the R-value, whereas in the other reference points the gradient has a fixed value.

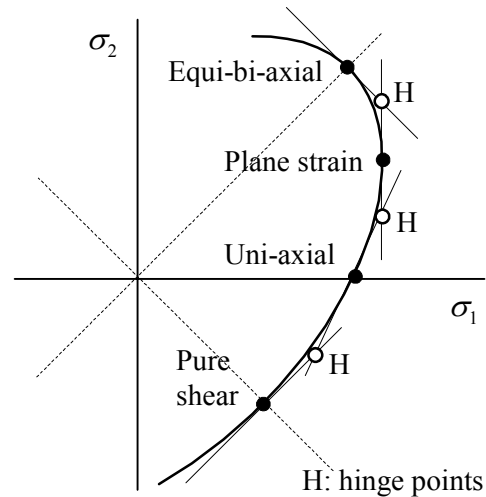


Figure 1 *The four reference points to construct the Vegter yield function in case of planar isotropy*

For the uni-axial point the R-value is defined according equation (1) and can be expressed in terms of $\dot{\epsilon}_1$ and $\dot{\epsilon}_2$ because of the plastic incompressibility:

$$R = \frac{\dot{\epsilon}_2}{\dot{\epsilon}_3} = \frac{\dot{\epsilon}_2}{-(\dot{\epsilon}_1 + \dot{\epsilon}_2)} \quad (1)$$

The gradient can be expressed in terms of the strain gradients which in turn can be

expressed in terms of the R-value according equation (2):

$$\frac{d\sigma_2}{d\sigma_1} = -\frac{\frac{\partial\phi}{\partial\sigma_1}}{\frac{\partial\phi}{\partial\sigma_2}} = -\frac{\dot{\varepsilon}_1}{\dot{\varepsilon}_2} = \frac{1+R}{R} \quad (2)$$

An overview of the gradients in case of planar isotropic material behaviour is given in Table 1.

Reference point	$d\sigma_2/d\sigma_1$
pure shear	1
uni-axial	$(1+R)/R$
plane strain	∞
equi-bi-axial	-1

Table 1 The gradient of the reference points in case of planar isotropic material behaviour.

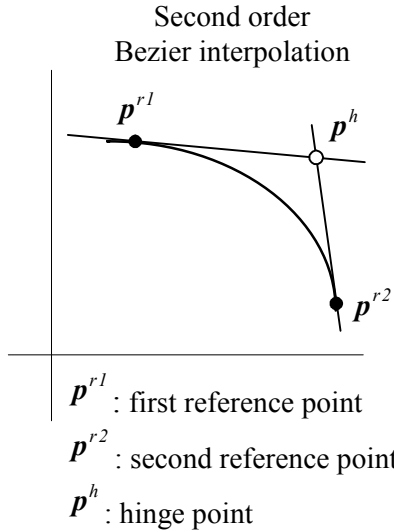


Figure 2 Second order Bezier interpolation with help of two reference points and one hinge point

A yield surface is constructed using the reference points and the gradients. This construction is performed with the help of Bezier interpolations. The hinge points p^h between the reference points p^{r1} and p^{r2} are defined as the intersection points of the gradients of the respective reference points. Between the reference points a second order Bezier interpolation is used, see Figure 2:

$$\sigma = (1-\beta)^2 p^{r1} + 2\beta(1-\beta)p^h + \beta^2 p^{r2} \quad (3)$$

Where β is a scalar increasing from 0 to 1 between the two reference points. For the four reference points, three Bezier interpolations are used to describe a quarter of the yield function. The first between the equi- bi-axial point and the plane strain point, the second between the plane strain point and the uni-axial point and the third between the uni-axial point and the pure shear point. This yield function is a multi-faceted yield function. The advantage of using Bezier interpolations is that the normal of the yield function is continuous in the reference points.

The major stresses σ_1 and σ_2 are defined in a way that $\sigma_1 \geq \sigma_2$. So only the part underneath the line $\sigma_1 = \sigma_2$ is needed. The material is assumed to behave identically under compression as under tension because of the lack of reliable compression tests. In case of planar isotropy, the yield surface is completed using symmetry in the line $\sigma_1 = -\sigma_2$. The construction of the yield surface can easily be extended to more points. The only condition is that the gradient must be known in that point. It is obvious that the yield surface must always remain convex.

2. PLANAR ISOTROPIC VEGTER YIELD FUNCTION

The stress definition of the yield surface is used to develop a yield function ϕ [3]. This Vegter yield function is defined as:

$$\phi = \sigma_{bez} - \sigma_y \quad (4)$$

Where σ_{bez} is a kind of equivalent stress and σ_y is the yield stress. In order to find a suitable expression for σ_{bez} , equation (3) is normalised with σ_{bez} . For both stress components the following expressions are found:

$$\frac{\sigma_1}{\sigma_{bez}} = (1-\beta)^2 p_1^{r1} + 2\beta(1-\beta)p_1^h + \beta^2 p_1^{r2}$$

$$\frac{\sigma_2}{\sigma_{bez}} = (1-\beta)^2 p_2^{r1} + 2\beta(1-\beta)p_2^h + \beta^2 p_2^{r2}$$
(5)

This results in two expressions for σ_{bez} :

$$\sigma_{bez} = \frac{\sigma_1}{(1-\beta)^2 p_1^{r1} + 2\beta(1-\beta)p_1^h + \beta^2 p_1^{r2}}$$

$$\sigma_{bez} = \frac{\sigma_2}{(1-\beta)^2 p_2^{r1} + 2\beta(1-\beta)p_2^h + \beta^2 p_2^{r2}}$$
(6)

With help of these expressions a quadratic function for β is found:

$$\beta^2(\sigma_2(p_1^{r2} - 2p_1^h + p_1^{r1}) - \sigma_1(p_2^{r2} - 2p_2^h + p_2^{r1}))$$

$$+ \beta(2\sigma_2(p_1^h - p_1^{r1}) - 2\sigma_1(p_2^h - p_2^{r1}))$$

$$+ \sigma_2 p_1^{r1} - \sigma_1 p_2^{r1} = 0$$
(7)

Only one value of β of equation (7) satisfies the boundary condition of lying between 0 and 1. The expression for σ_{bez} is found by substituting this value in one of the equations of (6).

The yield surface can be described with six Bezier interpolation functions because of the definition that $\sigma_1 \geq \sigma_2$, see Figure 3. The ratio σ_1/σ_2 determines the area where an Bezier interpolation is valid. Depending on the area, the reference points and the hinge points are defined. By substituting the right reference and hinge points into equation (6) the yield function can be determined. It must be noticed that σ_{bez} must be determined for every Bezier interpolation.

With the four reference points the yield function can be defined. The experiments to obtain the reference points must be performed at various angles with the rolling direction. When the reference points do not vary with the angle, the material behaves planar isotropic. Then the above mentioned description of the yield function is

satisfactory. But, when the reference points vary the material behaves planar anisotropic. In that case the yield function has to be extended.

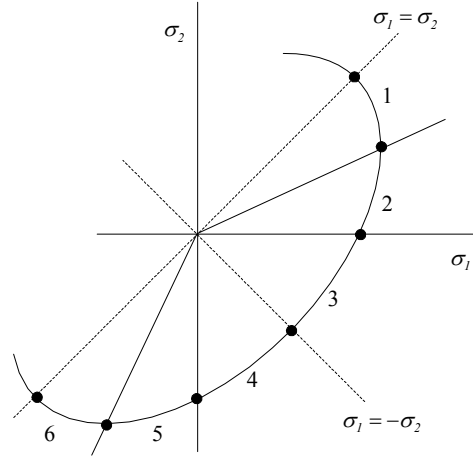


Figure 3 The six areas in the stress space of the Vegter yield function.

3. PLANAR ANISOTROPIC VEGTER YIELD FUNCTION

For four earing material the experiments are performed in three directions. These directions are related to the rolling direction and are described by the angle θ . The experiments are performed for $\theta = 0^\circ$, 45° and 90° . This is analogue to the determination of the Hill yield function [4]. So for each angle θ the reference points and R-value are obtained.

A yield surface for the measured angles θ can be constructed. The first part of the yield surface is constructed by using the measured reference points, the full circles in Figure 4. The yield surface can not be completed by simply using symmetry in the line $\sigma_1 = -\sigma_2$. Mirroring the reference points from the first part to the second part is accomplished with a shift in the rolling direction of 90° . So, for constructing the second part of the yield surface for the angle θ the reference points of the angle $\theta + 90^\circ$ must be used. The determination of the plane strain point in the second part of the yield surface is illustrated in Figure 4. The plane strain point for $\theta + 90^\circ$

is mirrored in the line $\sigma_1 = -\sigma_2$. The other reference points of the second part are also shown, the open circles in Figure 4.

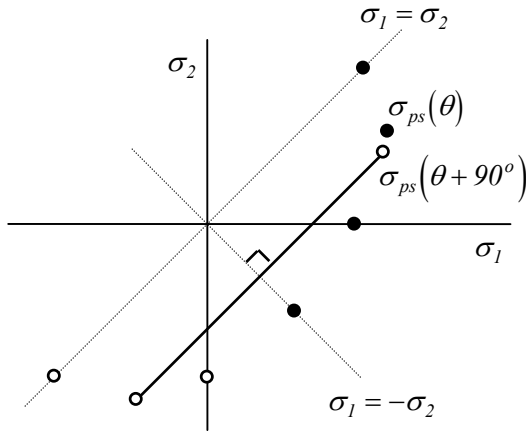


Figure 4 Construction of the reference points for the Vegter yield surface in case of planar anisotropy.

The gradients in the reference points also differ from the isotropic case. The stress state does not coincide with the deformation state because of the anisotropy. For example a equi-bi-axial stress state does not results in a equi-bi-axial deformation state. So, the gradient in each reference point must be constructed. This construction is explained for the equi-bi-axial point in Figure 5.

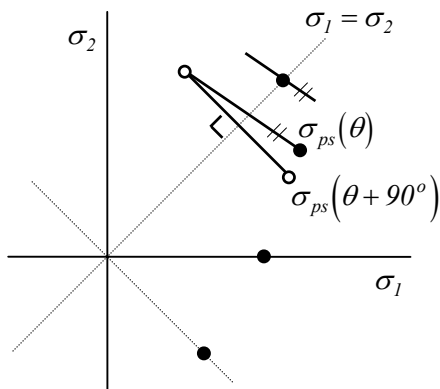


Figure 5 Construction of the gradients for the Vegter yield surface in case of planar anisotropy.

The gradient in the equi-bi-axial point can not be related to measurements. The desire of a smooth yield surface is the basis for the gradient construction. The gradient is constructed with help of the plane strain

point. The plane strain point for angle θ is drawn. The plane strain point for the angle $\theta + 90^\circ$ is mirrored in the line $\sigma_1 = \sigma_2$. The tangent in the equi-bi-axial point is defined parallel to the line between this two points.

The gradients in the plane strain point and in the uni-axial point are similar to the gradients in the isotropic case. The gradient in the pure shear point is constructed with help of the uni-axial points in a similar way as for the bi-axial point. An overview of the gradients in case of planar anisotropic material behaviour is given in Table 2.

Reference point	$d\sigma_2/d\sigma_1$
pure shear	$f(\sigma_{un}(\theta), \sigma_{un}(\theta + 90^\circ))$
uni-axial	$(1 + R(\theta)) / R(\theta)$
plane strain	∞
equi-bi-axial	$g(\sigma_{ps}(\theta), \sigma_{ps}(\theta + 90^\circ))$

Table 2 The gradient of the reference points in case of anisotropic material behaviour.

For the measured angles, a yield function based on second order Bezier interpolations is constructed. The yield function for an arbitrary angle can be determined with the help of an interpolation. The corresponding reference points are interpolated as a function of the angle θ to obtain a new reference point. With the interpolated reference points a new yield function can be constructed.

For the interpolation a suitable interpolation function must be found. The value of a reference point as function of the angle θ is denoted by $\sigma_{test}(\theta)$. The following boundary condition must be fulfilled; the angles $\theta=0^\circ$ and $\theta=90^\circ$ are angles of symmetry:

$$\sigma_{test}(\theta) = \sigma_{test}(-\theta) \quad (8)$$

$$\sigma_{test}(90^\circ - \theta) = \sigma_{test}(90^\circ + \theta)$$

This periodic function can be interpolated with a Fourier serie:

$$F(x) = \sum_{n=0}^{\infty} (a_n \sin nx + b_n \cos nx) \quad (9)$$

For four earing material this condition is met with the following terms of the Fourier serie:

$$\sigma_{test}(\theta) = A + B \cos 2\theta + C \cos 4\theta \quad (10)$$

The next boundary condition is rather obvious, the interpolation must correspond with the experimental value $\sigma_{exp,\theta}$:

$$\begin{aligned} \sigma_{test}(\theta = 0^\circ) &= \sigma_{exp,0} \\ \sigma_{test}(\theta = 45^\circ) &= \sigma_{exp,45} \\ \sigma_{test}(\theta = 90^\circ) &= \sigma_{exp,90} \end{aligned} \quad (11)$$

Equation (10) holds three unknowns which can be solved with the boundary condition (11). So, the interpolation function becomes:

$$\begin{aligned} \sigma_{test}(\theta) &= \frac{\sigma_{exp,0} + 2\sigma_{exp,45} + \sigma_{exp,90}}{4} + \\ &+ \frac{\sigma_{exp,0} - \sigma_{exp,90}}{2} \cos 2\theta + \\ &+ \frac{\sigma_{exp,0} - 2\sigma_{exp,45} + \sigma_{exp,90}}{4} \cos 4\theta \end{aligned} \quad (12)$$

With equation (12) it is possible to determine the reference points for arbitrary angles θ . With these reference points a Vegter yield function can be constructed. In Table 3 an example of the interpolation is given. The reference points are normalised by a mean yield stress. The columns $\theta = 0^\circ$, 45° and 90° represent the experimentally obtained values of the reference points and the R-value. The R-value must be interpolated to determine the gradient in the uni-axial point. With equation (12) the values for an angle of 30° with the rolling direction are derived. With the values printed in the last column, $\theta = 30^\circ$, the corresponding yield function can be constructed.

Experimental value	0°	45°	90°	θ
$\sigma_{pure\ shear}$	0.60	0.60	0.60	0.60

$\sigma_{uni-axial}$	0.90	1.10	1.00	1.04
$\sigma_{plane\ strain}$	1.10	1.25	1.15	1.21
$\sigma_{equi-biaxial}$	1.00	1.00	1.00	1.00
R-value	0.50	2.00	1.00	1.56

Table 3 The reference points and the R-values obtained from experiments (arbitrary normalised values) with interpolated values for $\theta = 30^\circ$.

4. APPLICATION

The Limiting Dome Height test (LDH) was used as a benchmark problem at the Numisheet '96 [5]. The LDH benchmark was designed to compare simulations and experiments for the prediction of failure and for the sensitivity of material behaviour. This application is very useful to examine the material description. The dimensions of the tool cross section at the line of symmetry are given Figure 6

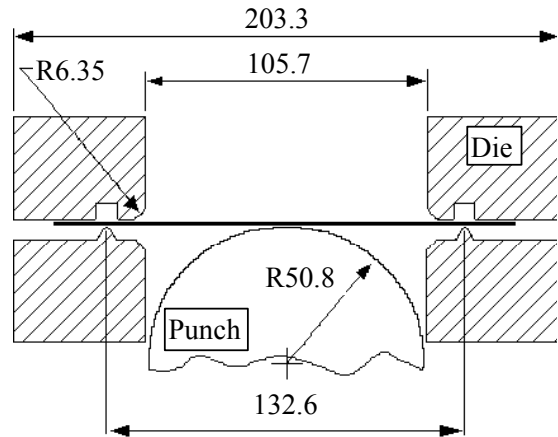


Figure 6 Schematic illustration of the LDH tools

For the LDH simulation only a quarter of the product is analysed because of symmetry. The quarter blank is shown in Figure 7. The x-axis and the y-axis are the axis of symmetry. The blank is meshed till the lockbead which is indicated at the right side. The lockbead is incorporated by an equivalent drawbead [6]. The equivalent drawbead works on the edge nodes at the right side of the blank. The top of the blank

is a free edge. The blank is modelled with 3000 plate elements.

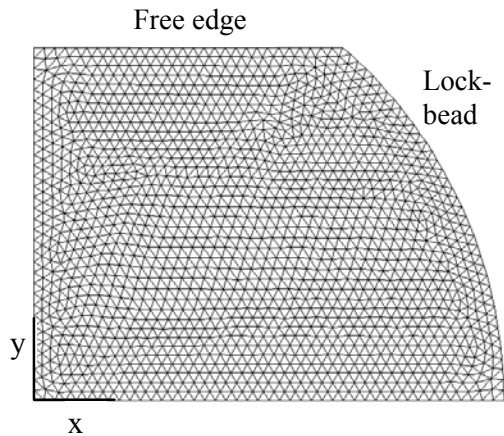


Figure 7 Original mesh with the position of the lockbead.

Three simulations are performed, every simulation uses a different material behaviour. The first simulation uses a planar isotropic Hill yield function. The second simulation uses a planar anisotropic Hill yield function whereas the third simulation uses a Vegter yield function. The material used is a draw quality mild steel. The stress strain curve is fitted with the Nadai formula. The parameters for the material descriptions are listed in Table 4. The material properties are obtained from experiments at Hoogovens Research & Development and can also be found in [3].

The reference points for the Vegter yield function are normalised with the yield stress. Because of the missing of experimental data for the pure shear point, this value is an estimated one. It is clearly that for the Vegter yield function much more parameters are necessary. So, to use this function an extensive experimental program must be performed.

E N/mm ²	ν	σ_{yield} N/mm ²	C	n
206000	0.3	158	520	0.233

Vegter :	0°	45°	90°
pure shear	0.545	0.545	0.545
uni-axial	0.993	1.009	0.991
plane strain	1.233	1.228	1.262

equi-biaxial	1.190	1.190	1.190
R	2.07	1.86	2.63

Table 4 Material properties for the LDH simulation.

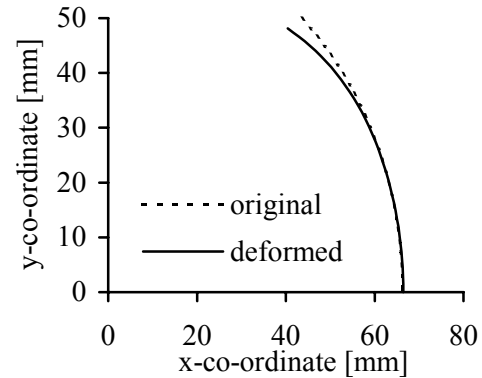


Figure 8 Draw-in at the lockbead

A first interesting point is the draw-in at the lock bead. The coordinate of the lockbead edge of the original blank and of the deformed blank are printed in Figure 8. The dotted line represents the original position of the lockbead edge and the full line represents the position of the points which originally started in the lockbead. All three simulations show an identical draw-in, so only one deformed edge is printed.

As can be seen, the lockbead not fully locks the material. At the axis of symmetry the material is locked whereas at the free edge the material draw-in is about 4.5 mm. A draw-in at the free edge was also found in the experiments. So, the approximation of the lockbead with the equivalent drawbead is better than completely lock the lockbead edge.

The major and minor strains along the x-axis are presented in Figure 9 and Figure 10 respectively. The average results of the Numisheet experimental benchmark participants are also presented in these graphs. The strains are evaluated at the outer side of the product away from the punch.

Looking at the major strain, the maximum value is found at a x-coordinate of 30 mm. For larger x-coordinates the three simulations show a smaller value than the experiments. For smaller x-coordinates the

planar isotropic Hill description shows smaller strain values whereas the planar anisotropic Hill description shows larger values. The Vegter description lies between the two simulations with the Hill description and compares very well with the experiments.

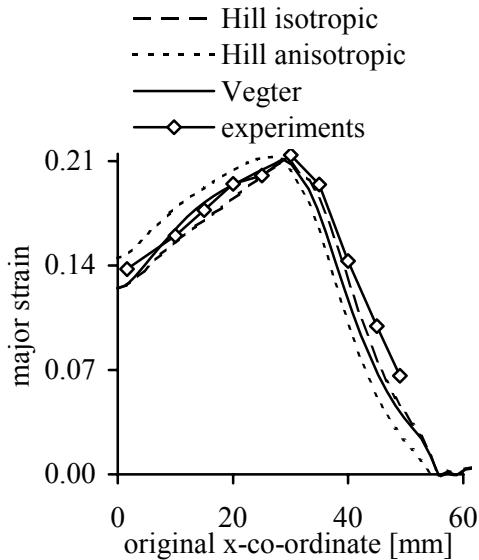


Figure 9 Major strain along the x-axis

Looking at the minor strain, the Vegter description again compares very well with the experiments. The two simulations with the Hill description show more strain and clearly deviate from the experiments.

The deformations on the x-axis lie between the uni-axial point and the plane strain point. The position of the plane strain point is of importance to describe the deformations on the x-axis. The Vegter yield function is constructed using among others the plane strain point whereas the Hill yield function only uses the uni-axial point. This is the strength of the Vegter yield function and the reason that this yield function gives a better description of the strains. The extensive experimental program is worth while when an accurate description of the material behaviour is needed.

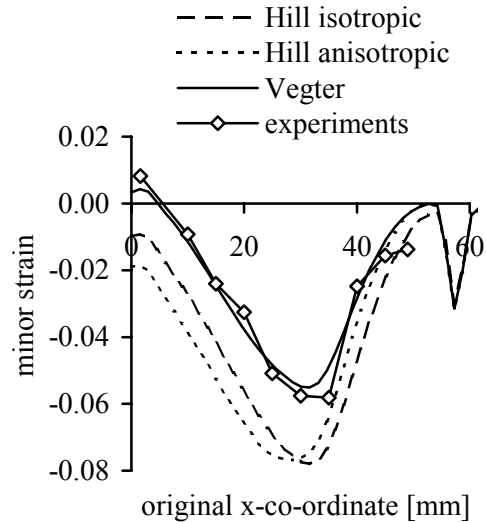


Figure 10 Minor strain along the x-axis.

The Forming Limit Diagram (FLD) of this mild steel is used to predict failure. In an FLD two areas can be distinguished. The Forming Limit Curve (FLC) divides the strain space into a safe part and a failure part. The strain combinations below the FLC are in the safe part and above the FLC are in the failure part.

Figure 11 shows the FLD for the draw quality mild steel. In this figure also the strains of the LDH simulation with the Vegter material at a punch height of 40.05 mm are shown. It is clear that most strain combinations are in the safe zone but a few strain combinations just pass the line of the FLC. So, the material fails at a punch height of 40.05 mm. The failure zone is at the line of symmetry, at the x-axis.

The average value of the Numisheet experimental benchmark participants was 40.1 mm. So, the simulation predicts the punch height at failure very well. It should be mentioned that the spread in the experimental results was rather large. The minimum value was 30.0 mm whereas the maximum value was 46.0 mm.

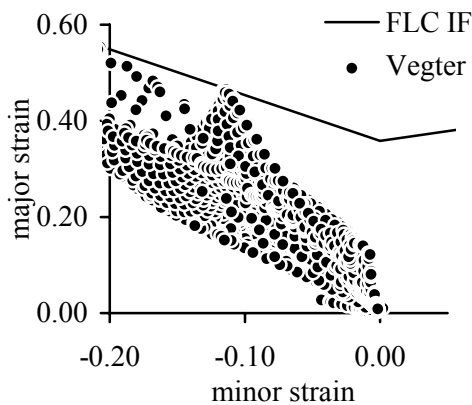


Figure 11 *Forming limit diagram for the LDH at a punch height of 40.05 mm.*

5. CONCLUSIONS

The material model is of a major importance for a reliable finite element simulation. The Vegter yield function uses multi-axial stress states to describe the material behaviour whereas the classical Hill yield function only uses the uni-axial stress state.

The Limiting Dome Height test was used to demonstrate the influence of the material description. The Vegter yield function has proved to give an accurate description of the strain distribution and of the punch height at failure.

For the Vegter yield function an extensive set of experimental parameters is needed. Hence, when an accurate description of the material behaviour is needed the extensive experimental program is worth while.

REFERENCES

- [1] R. Hill, *The mathematical theory of plasticity*, Clarendon Press, Oxford, 1950
- [2] H. Vegter, P. Drent, J. Huétink, *A planar isotropic yield criterion based on mechanical testing at multi-axial stress states*, Simulation of materials processing: theory, methods and applications, S. F. Shen & P. Dawson (eds.), Balkema, Rotterdam, 1995
- [3] H.H. Pijlman, *Implementation of the*

Vegter yield criterion in the finite element program DIEKA, graduate report, University of Twente, 1996

- [4] D.W.A. Rees, *Equivalence and instability correlations for isotropic and anisotropic sheet plasticity*, J. of Mat. Proc. Tech., 40, 1994
- [5] Numisheet '96, Numerical simulations of 3-D sheet metal forming processes, verification of simulations with experiments, J.K. Lee et al. (eds.), 1996
- [6] B.D. Carleer, T. Meinders, J. Huétink, *Equivalent drawbead model in finite element simulations*, Numerical simulations of 3-D sheet metal forming processes, verification of simulations with experiments, J.K. Lee et al. (eds.), 1996